Self-sustained lift and low friction via soft lubrication

Baudouin Saintyves[a,1], Theo Jules[a,b,1], Thomas Salez[a,c], and L. Mahadevan[a,d,e,f,g,2]

[a]Paulson School of Engineering and Applied Sciences, Harvard University, Cambridge, MA 02138; [b]Department de Physique, École Normale Supérieure, Université de Recherche Paris Sciences et Lettres, 75005 Paris, France; [c]Laboratoire de Physico-Chimie Théorique, UMR CNRS 7083 Gulliver, École Supérieure de Physique et de Chimie Industrielles de la Ville de Paris, Université de Recherche Paris Sciences et Lettres, 75005 Paris, France; [d]Department of Physics, Harvard University, Cambridge, MA 02138; [e]Department of Organismic and Evolutionary Biology, Harvard University, Cambridge, MA 02138; [f]Wyss Institute for Biologically Inspired Engineering, Harvard University, Cambridge, MA 02138; and [g]Kavli Institute for Bionano Science and Technology, Harvard University, Cambridge, MA 02138

Edited by Steve Granick, IBS Center for Soft and Living Matter, Ulju-gun, Ulsan, South Korea, and approved March 25, 2016 (received for review December 23, 2015)

Relative motion between soft wet solids arises in a number of applications in natural and artificial settings, and invariably couples elastic deformation fluid flow. We explore this in a minimal setting by considering a fluid-immersed negatively buoyant cylinder moving along a soft inclined wall. Our experiments show that there is an emergent robust steady-state sliding regime of the cylinder with an effective friction that is significantly reduced relative to that of rigid fluid-lubricated contacts. A simple scaling approach that couples the cylinder-induced flow to substrate deformation allows us to explain the elastohydrodynamic lift that underlies the self-sustained lubricated motion of the cylinder, consistent with recent theoretical predictions. Our results suggest an explanation for a range of effects such as reduced wear in animal joints and long-runout landslides, and can be couched as a design principle for low-friction interfaces.

lubrication | friction | elastohydrodynamics | soft contact

Sliding motion between contacting solids arises in a range of phenomena that spans many length scales and timescales, and includes landslides (1), aquaplaning of tires (2), industrial bearings (3), synovial and cartilaginous joints (4–8), cell motion in blood vessels and microfluidic devices (9–12), and atomic-force and surface force rheological apparatuses (13). Interfacial sliding invariably involves friction and adhesion, as well as fluid lubrication and elastic deformation (14, 15).

Since the pioneering work of Reynolds (16), fluid lubrication has been extensively studied, initially in the context of heavy industry (3), and more recently in the context of motion at soft material and biological interfaces (17). In heavy-load, high-velocity settings, strongly confined induced viscous flows can generate high pressure and heat, with associated rheological piezoviscous, thermoviscous effects and nanometric substrate deformations (3). In contrast, in light loading conditions associated with steady sliding motions at soft wet interfaces, the coupling between elasticity and flow leads to long wavelength deformations that predict the emergence of lift and reduced friction (18–21). Perhaps surprisingly, it is only recently that the problem of a free particle that can simultaneously sediment, slide, or roll has been treated (22), with further predictions of a range of counterintuitive solutions such as enhanced sedimentation, bouncing, roll reversal, and self-sustained long-runout sliding. Here, we consider a minimal experimental setting to test these predictions, and focus in particular on the self-sustained elastohydrodynamic lift and the accompanying low effective friction associated with the motion of a heavy fluid-immersed cylinder sliding along a soft inclined wall.

Our setup, sketched in Fig. 1*A*, consists of a glass plate ($0.5 \times 5 \times 30$ cm) mounted on a variable incline (angle α), coated with a thin layer of soft material [polyacrylamide (PAA) or polydimethylsiloxane (PDMS) with varying cross-linker and monomer concentrations (*SI Appendix*)] of thickness h and shear modulus G, immersed in a transparent aquarium ($8 \times 15 \times 33$ cm) filled with Rhodorsil silicone oil of density $\rho_{\text{oil}} = 970$ kg/m^3 and with varying viscosities η. Cylinders of radii R, made of different materials of density ρ (relative density $\rho^* = \rho - \rho_{\text{oil}} > 0$), are allowed to slide down the incline after being launched manually, and their trajectory is followed using a simple wide-angle camera. To visualize the profile of the deformed coating, we embed fluorescent polyethylene particles at the elastic–oil interface, use a blue laser sheet to illuminate the interface from below, and focus a near-field macrolens on the interface, as shown in Fig. 1*A*; this allows us to see only the interface (Fig. 1*B* and Movie S1). In a given experiment, we observe both spinning and sliding motions of the cylinder (Movie S2), so that the translation speed is $\dot{\theta}R + V$, where $\dot{\theta}$ is the angular velocity and V is the sliding speed. For most experiments, $V \gg R\dot{\theta}$ (except for motion near very soft substrates, with $G <$ 1,000 Pa), and thus we focus on the sliding motion that is extracted via an image-processing algorithm.

For a baseline, we first perform experiments with the cylinder moving down a rigid glass incline, and see stick–slip motion dominated by surface roughness (23), rather than fluid-lubricated smooth motion of the cylinder considered theoretically (24, 25); the dotted line in Fig. 2*A* highlights this intermittent low-speed motion that is very sensitive to initial conditions. When the cylinder moves on a soft coating, its motion transitions to that dominated by fluid-lubricated contact and there are a number of new effects. First, we observe that, for certain combinations of cylinder size and density, the cylinder reverses its rolling direction (Movie S3), consistent with recent predictions (22). Second, we observe damped oscillations (Movie S4) when the cylinder is launched from a large height and it settles into its steady-state sliding motion, as predicted in ref. 22. Most strikingly, over a robust range of parameters, we see a steady sliding of the cylinder

Significance

Contacting solids that move relative to each other in a fluid environment abound in many settings such as soft contact lenses in eyes, animal joints, and bearings in rotating machinery. Motion is inevitably accompanied by flow and deformation, and raises the question of how these correlate with friction at the interface. A minimal experimental setting, associated with how a cylinder slides and rolls along a soft inclined plane, allows us to see the induction of a self-sustained lift that reduces the friction by nearly an order of magnitude. A simple scaling theory explains our results and suggests a design principle for low-friction interfaces and a partial explanation for phenomena such as reduced wear in animal joints and long-runout landslides.

Author contributions: B.S., T.S., and L.M. designed research; B.S., T.J., T.S., and L.M. performed research; B.S. and T.J. contributed new reagents/analytic tools; B.S., T.J., T.S., and L.M. analyzed data; and B.S., T.S., and L.M. wrote the paper.

The authors declare no conflict of interest.

This article is a PNAS Direct Submission.

[1]B.S. and T.J. contributed equally to this work.

[2]To whom correspondence should be addressed. Email: lm@seas.harvard.edu.

This article contains supporting information online at www.pnas.org/lookup/suppl/doi:10.1073/pnas.1525462113/-/DCSupplemental.

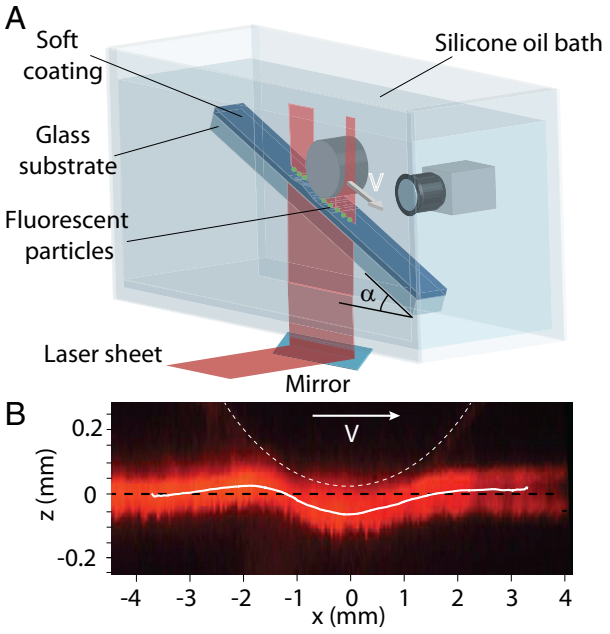

Fig. 1. Experimental setup and laser profilometry. (*A*) A negatively buoyant rigid cylinder immersed in a viscous bath slides down a tilted wall that is coated with a thin elastic layer. Fluorescent particles embedded in the latter allow for laser profilometry of the elastic layer–oil interface. (*B*) Side view of the substrate deformation (red) obtained with the laser sheet. The center of the cylinder is located at $x = 0$. The white dashed line is a guide to the eye indicating the cylinder profile; the black dashed line corresponds to the unperturbed state of the substrate. The white solid line corresponds to the center of the fluorescent signal from the particles, obtained by using a transverse Gaussian fit, showing the asymmetric profile of the elastic layer–oil interface. The experimental parameters are $G = 65$ kPa, $h = 1.5$ mm, $\eta = 1$ Pa·s, $R = 12.7$ mm, $\rho = 8{,}510$ kg/m^3, and $\alpha = 11°$.

accompanied by an asymmetrically deformed elastic–oil interface (Movie S1), as shown in Fig. 1*B*. This counterintuitive observation suggests a mechanism for self-sustained lift at soft wet interfaces with implications for a range of phenomena that go beyond the simple instantiation here.

A simple modification of classical lubrication theory (16, 26) allows us to understand this result qualitatively. For the case of rigid interfaces, the fore–aft symmetry of the gap implies that the pressure field is antisymmetric with a null normal resultant force. However, when the wall or cylinder is soft, this pressure asymmetry leads to an asymmetric elastic deformation (18–20, 22) that generates lift dynamically, and is capable of sustaining the cylinder's weight. Consistent with this, independent of initial conditions, over the entire range of tested substrate thicknesses and moduli, the cylinder achieves a robust sliding steady state (Fig. 2*A*) with a speed that is substantially higher than its speed when sliding along a rigid glass wall. The same behavior is also qualitatively observed for elliptical cylinders (*SI Appendix* and Movie S5)—because these do not spin, we can disregard rotation as the primary origin of self-sustained lift and reduced friction. Moving to quantify the role of the soft substrate, we note that the thicker (Fig. 2*A*) and the softer (Fig. 2*B*) the elastic layer, the higher the sliding speed, up to a certain point. In Fig. 2*B*, we see that the sliding speed is a nonmonotonic function of the modulus; it falls off for large moduli as expected, but also for small moduli owing to effects such as large substrate deformations (see Movie S6 for an example of an experiment with a very soft coating).

To minimally quantify the emergence of self-sustained lift and sliding motion of the cylinder at speed V, we limit ourselves to considerations of small strains in the elastic layer; as we will see, this suffices to explain most of our experiments. Assuming that the cylinder of radius R is separated from the undeformed substrate by a minimum gap $\delta \ll R$, the tangential size of the contact zone scales as $l \sim \sqrt{R\delta}$, so that $\delta \ll l \ll R$. This separation of scales allows us to invoke lubrication theory (26). Then, the flow-induced pressure p scales as $p \sim \eta V l/(\delta + \Delta h)^2$, where $\Delta h \sim h\, p/G \ll h$ is the normal elastic deformation of the soft layer (19, 27). Together, this implies that the elastohydrodynamic pressure scales as $\eta^2 V^2 R h/(G\delta^4)$ at leading order. Integrating this pressure over the contact length l leads to a positive elastohydrodynamic lift force per unit length that scales as $\sim \eta^2 V^2 R^{3/2} h/(G\delta^{7/2})$ (19, 20).

At steady state, $V = V_\infty$, the elastohydrodynamic lift normal to the incline must balance the normal projection of the cylinder weight $\sim \rho^* g R^2 \cos\alpha$, whereas the tangential gravitational driving power $\sim V_\infty \rho^* g R^2 \sin\alpha$ must balance the resisting viscous power $\sim \eta (V_\infty/\delta)^2 l\delta$. These relations yield the theoretical steady-state sliding speed:

$$V_\infty^{\text{th}} = A \frac{\rho^* g R^2 \sin\alpha}{\eta} \left(\frac{\rho^* g h \cos\alpha}{G}\right)^{1/5} \left(\frac{\sin\alpha}{\cos\alpha}\right)^{2/5}, \qquad [1]$$

where A is a dimensionless constant. We note that V_∞^{th} is the Stokes velocity $\sim \rho^* g R^2 \sin\alpha/\eta$ of a particle of size R in an infinite fluid, modified by the effect of elastohydrodynamics; indeed, the

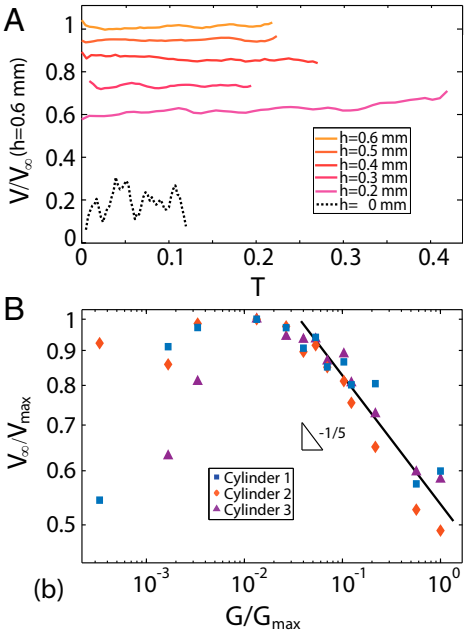

Fig. 2. Sliding speed as a function of time and shear modulus of the substrate. (*A*) Sliding speed V of an aluminum cylinder as a function of normalized time $T = tV_\infty/d$, for different thicknesses h of the soft coating. Here, V_∞ is the time-averaged steady-state sliding speed, d is the total length of the substrate, and t is the time. The vertical axis is normalized by V_∞ (for $h = 0.6$ mm). The dotted line corresponds to the case of a bare glass substrate, whereas the solid lines are for coatings with an elastic layer of shear modulus $G = 31$ kPa. The other experimental parameters are $\rho = 2{,}720$ kg/m^3, $R = 12.7$ mm, $\eta = 1$ Pa·s, and $\alpha = 11°$. (*B*) Time-averaged steady-state sliding speed for three different cylinders as a function of the shear modulus of the coating, with thickness $h = 600$ μm, oil bath viscosity $\eta = 1$ Pa·s, and angle $\alpha = 11°$. The vertical axis is normalized by the maximum steady-state sliding speed $V_{\max}$ for the corresponding cylinder. The horizontal axis is normalized by the maximum of the tested moduli $G_{\max} = 300$ kPa. The solid line has a slope of $-1/5$ (Eq. **1**). The other parameters are as follows. Cylinder 1 (aluminum): $\rho = 2{,}720$ kg/m^3, $R = 12.7$ mm; cylinder 2 (glass): $\rho = 2240$ kg/m^3, $R = 9.5$ mm; cylinder 3 (brass): $\rho = 8{,}510$ kg/m^3, $R = 6.35$ mm.

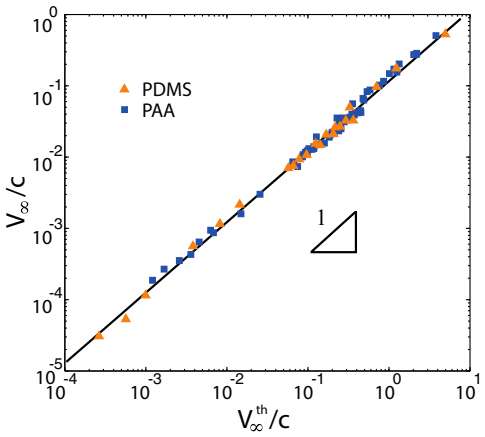

Fig. 3. Master curve for steady sliding speed of an immersed cylinder on a soft substrate. Time-averaged steady-state sliding speed V_∞ (Fig. 2) as a function of its theoretical prediction V_∞^{th} (Eq. **1**). Both axes are scaled by the free fall speed $c=\sqrt{2gR\rho^*/\rho}$. The experiments were performed using either PDMS elastomers (triangles) or PAA hydrogels (squares). Both materials give overlapping results for a range of moduli. The solid line has unit slope.

steady-state gap reads $\delta_\infty \sim R(\rho^* gh\cos\alpha/G)^{2/5}(\sin\alpha/\cos\alpha)^{4/5}$ and allows us to rewrite the above scaling law in terms of the gap under more general loading conditions. A first check of Eq. **1** can be seen already in Fig. 2 showing evidence of the steady speed for a range of elastic layer thicknesses and moduli; furthermore, the speed is inversely proportional to $G^{1/5}$ in the small deformation limit, i.e., for relatively stiff materials. To test Eq. **1** further, we used cylinders (all of width 12.7 mm) with radii $R=12.7$, 9.5, and 6.35 mm, and densities $\rho=8{,}510$, 2,720, and 2,240 kg/m^3 corresponding to brass, aluminum, and glass, moving in fluids with a range of viscosities $\eta=0.01$, 0.35, 1, 30, and 100 Pa·s, along an incline with angle $\alpha\in[10°-40°]$, that is coated with two different soft materials (PDMS, PAA) of modulus $G\in[8-300]$ kPa [independently measured using a CP50 cone-plate geometry in an MCR 501 Anton Paar rheometer (*SI Appendix*)] and thickness $h\in[100\ \mu\text{m}-2\ \text{mm}]$. In Fig. 3, we see that the measured sliding speed is in excellent agreement with Eq. **1**, over five decades in the scaled speed for both PDMS and PAA materials. Furthermore, the experimental prefactor $A=0.12\pm0.02$ in Eq. **1** is consistent with the theoretical prediction $A\approx0.2$ (22).

Although Eq. **1** captures the small-deformation regime associated with self-sustained lift and low friction, it cannot explain the decreasing of the sliding speed when the substrate is very soft, as shown in Fig. 2*B*, that is, when $\Delta h/h\geq10\%$. In this situation associated with large deformations, we need a nonlinear extension of the present theory (20). However, it is worth noting that steady-state sliding is still observed in this regime and the sliding speed remains larger than in the case of a rigid substrate, suggesting that the lift force remains important even here.

Our study of the motion of a fluid-immersed cylinder on a soft incline shows how self-sustained lift and low friction emerge dynamically due to the asymmetric elastic deformation induced by the lubrication flow in the contact zone, in quantitative agreement with a recent theory (22). The origin of the low friction is the viscous-flow–induced fore–aft asymmetry of the deformation profile of the incline, and leads to an elastohydrodynamic analog of Reynolds slider bearing (16). This yields a scaling law for the steady velocity as a function of the fluid viscosity, the elastic modulus and thickness of the substrate, gravity, inclination angle, and the size of the particle, which we corroborate using experiments. These observations, when combined with substrate poroelasticity (19), may partly explain a variety of phenomena that couple flow and deformation at soft interfaces such as long-runout landslides (1) or low friction and wear of synovial joints (5). Our study also points to a simple design principle for the reduction of friction and wear at soft interfaces, by tuning the elastohydrodynamic interaction between soft particles using their shape and deformation properties, and might allow us to design fluid suspensions with controllable rheologies.

ACKNOWLEDGMENTS. We thank Shmuel Rubinstein for help with imaging, Jun Chung for discussions, and the MacArthur Foundation (L.M.) and the Harvard Materials Research Science and Engineering Center (Grant DMR-1420570) for partial financial support.

1. Campbell CS (1989) Self-lubrication for long runout landslides. *J Geol* 97:653–665.
2. Brochard-Wyart F (2003) Hydrodynamics at soft surfaces: From rubber tyres to living cells. *Compt Rend Phys* 4(2):207–210.
3. Hamrock BJ, ed (1994) *Fundamentals of Fluid Film Lubrication* (McGraw-Hill, New York).
4. Maroudas AI (1976) Balance between swelling pressure and collagen tension in normal and degenerate cartilage. *Nature* 260(5554):808–809.
5. Greene GW, et al. (2011) Adaptive mechanically controlled lubrication mechanism found in articular joints. *Proc Natl Acad Sci USA* 108(13):5255–5259.
6. Grodzinsky AJ, Lipshitz H, Glimcher MJ (1978) Electromechanical properties of articular cartilage during compression and stress relaxation. *Nature* 275(5679):448–450.
7. Mow VC, Guo XE (2002) Mechano-electrochemical properties of articular cartilage: Their inhomogeneities and anisotropies. *Annu Rev Biomed Eng* 4:175–209.
8. Mow VC, Holmes MH, Lai WM (1984) Fluid transport and mechanical properties of articular cartilage: A review. *J Biomech* 17(5):377–394.
9. Goldsmith HL (1971) Red cell motions and wall interactions in tube flow. *Fed Proc* 30(5):1578–1590.
10. Byun S, et al. (2013) Characterizing deformability and surface friction of cancer cells. *Proc Natl Acad Sci USA* 110(19):7580–7585.
11. Higgins JM, Eddington DT, Bhatia SN, Mahadevan L (2007) Sickle cell vasoocclusion and rescue in a microfluidic device. *Proc Natl Acad Sci USA* 104(51):20496–20500.
12. Cohen SIA, Mahadevan L (2013) Hydrodynamics of hemostasis in sickle-cell disease. *Phys Rev Lett* 110(13):138104.
13. Villey R, et al. (2013) Effect of surface elasticity on the rheology of nanometric liquids. *Phys Rev Lett* 111(21):215701.
14. Persson BNJ (2000) *Sliding Friction* (Springer, New York).
15. Persson BNJ, Scaraggi M (2009) On the transition from boundary lubrication to hydrodynamic lubrication in soft contacts. *J Phys Condens Matter* 21(18):185002.
16. Reynolds O (1886) On the theory of lubrication and its application to Mr. Beauchamp Tower's experiments, including an experimental determination of the viscosity of olive oil. *Proc R Soc Lond* 40(242-245):191–203.
17. Zeng H, ed (2013) *Polymer Adhesion, Friction and Lubrication* (Wiley, Hoboken, NJ).
18. Sekimoto K, Leibler L (1993) A mechanism for shear thickening of polymer-bearing surfaces: Elasto-hydrodynamic coupling. *Europhys Lett* 23:113.
19. Skotheim JM, Mahadevan L (2004) Soft lubrication. *Phys Rev Lett* 92(24):245509.
20. Skotheim JM, Mahadevan L (2005) Soft lubrication: The elastohydrodynamics of nonconforming and conforming contacts. *Phys Fluids* 17:092101.
21. Snoeijer JH, Eggers J, Venner CH (2013) Similarity theory of lubricated Hertzian contacts. *Phys Fluids* 25:101705.
22. Salez T, Mahadevan L (2015) Elastohydrodynamics of a sliding, spinning and sedimenting cylinder near a soft wall. *J Fluid Mech* 779:181–196.
23. Bowden FP, Tabor D (1973) *Friction: An Introduction to Tribology* (Anchor, Garden City, NY).
24. Brenner H (1962) Effect of finite boundaries on the Stokes resistance of an arbitrary particle. *J Fluid Mech* 12:35–48.
25. Jeffrey DJ, Onishi Y (1981) The slow motion of a cylinder next to a plane wall. *Q J Mech Appl Math* 34:129–137.
26. Batchelor GK (1967) *An Introduction to Fluid Dynamics* (Cambridge Univ Press, Cambridge, UK).
27. Johnson KL (1985) *Contact Mechanics* (Cambridge Univ Press, Cambridge, UK).